Evaluation of the intramammary distribution of breast lesions detected by MRI but not conventional second-look B-mode ultrasound using an MRI/ultrasound fusion technique

Masayuki Saito[1], Hirona Banno[1], Yukie Ito[1], Mirai Ido[1], Manami Goto[1], Takahito Ando[1], Yukako Mouri[1], Junko Kousaka[1], Kimihito Fujii[1], Tsuneo Imai[1], Shogo Nakano[1*] and Kojiro Suzuki[2]

Abstract

The objective of this study was to evaluate the intramammary distribution of MRI-detected mass and focus lesions that were difficult to identify with conventional B-mode ultrasound (US) alone. Consecutive patients with lesions detected with MRI but not second-look conventional B-mode US were enrolled between May 2015 and June 2023. Following an additional supine MRI examination, we performed third-look US using real-time virtual sonography (RVS), an MRI/US image fusion technique. We divided the distribution of MRI-detected mammary gland lesions as follows: center of the mammary gland versus other (superficial fascia, deep fascia, and atrophic mammary gland). We were able to detect 27 (84%) of 32 MRI-detected lesions using third-look US with RVS. Of these 27 lesions, 5 (19%) were in the center of the mammary gland and 22 (81%) were located in other areas. We were able to biopsy all 27 lesions; 8 (30%) were malignant and 19 (70%) were benign. Histopathologically, three malignant lesions were invasive ductal carcinoma (IDC; luminal A), one was IDC (luminal B), and four were ductal carcinoma in situ (low-grade). Malignant lesions were found in all areas. During this study period, 132 MRI-detected lesions were identified and 43 (33%) were located in the center of the mammary gland and 87 (64%) were in other areas. Also, we were able to detect 105 of 137 MRI-detected lesions by second-look conventional-B mode US and 38 (36%) were located in the center of the mammary gland and 67 (64%) were in other areas. In this study, 81% of the lesions identified using third-look US with RVS and 64% lesions detected by second-look conventional-B mode US were located outside the center of the mammary gland. We consider that adequate attention should be paid to the whole mammary gland when we perform third-look US using MRI/US fusion technique.

Keywords Real-time virtual sonography, MRI-detected lesion, Second-look ultrasound, Third-look ultrasound, Breast cancer

*Correspondence:
Shogo Nakano
snakano1@aichi-med-u.ac.jp
Full list of author information is available at the end of the article

Saito *et al. BMC Medical Imaging*   (2024) 24:200

Page 2 of 11

Background

Magnetic resonance imaging (MRI) of the breast is a useful tool for detecting breast cancer. MRI is increasingly used to assess symptoms, screen women at high risk for breast cancer, stage known breast cancers, and screen the contralateral breast in patients with newly diagnosed breast cancer [1, 2]. Several authors have questioned the utility of preoperative MRI, given the possibility of overdiagnosis or false-positives [3, 4]. However, others have reported that MRI can reliably predict tumor progression, especially in very dense breasts [5].

The specificity and moderate positive predictive value of MRI can limit its effectiveness. A recent meta-analysis about using preoperative MRI to detect multifocal or multicentric cancers in the ipsilateral breast showed that the rate of additional cancer foci being detected ranged from 6 to 34%; the median was 16% and the positive predictive value was 66% [6]. Thus, breast biopsy is necessary in order to definitively diagnose suspicious lesions, especially in MRI-detected lesions that are not detected on initial mammography and ultrasound (US). When lesions detected with MRI are also detected with second-look US, US-guided biopsy is recommended.

Second-look US has detection rates that vary substantially [7–11]. Moreover, it is difficult to identify all lesions because examination success depends on the sonographer's experience and skill. Furthermore, lesion characterization with breast US has not reproducible among examiners, which remains a clinical challenge.

MRI-guided biopsy has been developed over the past several years to help diagnose conventional B-mode–occult breast lesions detected with MRI. Compared with other modalities, MRI-guided biopsies are less accurate [12–14]. Moreover, target sampling is more difficult after MRI-guided biopsy than after biopsy with ultrasound or stereotactic guidance. Radiopathologic correlation after MRI-guided biopsy is particularly challenging when MRI lesions only enhance in vivo and their presence cannot be confirmed in the biopsy specimen, even when biopsy markers have been appropriately placed [12].

Real-time virtual sonography (RVS) is an MRI/US image fusion technique introduced in 2005. RVS combines real-time sonography with MRI, allowing for the display of images from both imaging modalities on the same monitor. During sonography, the RVS system identifies the probe's position and movement. It simultaneously reconstructs an equivalent MRI image from previously imported volume data. If a lesion that was initially detected with prone MRI cannot be identified during second-look conventional B-mode US, we add supine MRI and perform second-look US using RVS (third-look US using RVS in this study). Regarding breast deformation, tumor displacement during MRI results from discrepancies between positions during supine versus prone examination [8, 15–17].

Satake et al. reported that tumor displacement in the breast during MRI due to prone versus supine positioning varies by tumor location. It is most common in the inner lower quadrant [18]. Carbonaro et al. reported that lesion-to-nipple distance might be the most reliable measure for second-look breast US [19]. However, few studies have examined the intramammary distribution of MRI-detected lesions in detail by dividing them into zones with third-look US using RVS. In the report by Nakano et al., supine MRI was performed first and prone MRI was not mandatory [16]. In this study, prone MRI was performed first, and when MRI-detected lesions were detected, supine MRI was added and third-look US using RVS was performed. The protocol of this study was different from that of Nakano et al. [16] in this regard, and we decided to validate the distribution of MRI-detected lesions with this protocol. The objective of this study was to evaluate the intramammary distribution of MRI-detected mass and focus lesions that were difficult to identify with conventional B-mode US alone.

Methods

Patients and lesions

This study was approved by the institutional review board of Aichi Medical University Hospital (No. 2022–125). The need for written informed consent was waived for this research study. Consecutive patients with one or more MRI-detected lesions that were not identified with second-look conventional B-mode US between May 2015 and June 2023 were enrolled in this study. Third-look US using RVS was performed to identify these lesions. Non–mass enhancement (NME) was excluded from this study because of the difficulty in objectively assessing them. US-guided biopsy was performed for MRI-detected lesions detected with RVS; additional excisional biopsy was performed if necessary.

Prone MRI

Prone MRI was used for preoperative assessment or to evaluate abnormal findings further. A dedicated double-breast coil was used with a 1.5-T scanner (Magnetom, Siemens Medical Systems, Erlangen, Germany) [20].

Second-look conventional B-mode US

After prone MRI, a 13-MHz linear array probe (HI VISION Ascendus, ARIETTA 850; FUJIFILM Health care Corporation, Japan) was used for second-look conventional B-mode US with the patient in the supine and arm-up position [20]. It was performed by experienced surgeons routinely involved in breast cancer treatment regardless of the experiences of third-look US using RVS.

Saito *et al. BMC Medical Imaging*   (2024) 24:200

Page 3 of 11

Supine MRI

When a lesion initially detected with prone MRI was not identified with second-look conventional B-mode US, supine MRI was added to acquire the data necessary for US using RVS. Supine MRI with a 1.5-T scanner (Magnetom, Siemens Medical Systems) was performed with the arm raised [20]. A flexible body surface coil was used to achieve the same position as that used in US [15, 20]. Acquisition was performed as described previously. We evaluated the lesion size, type (focus, mass, or NME), shape (oval, round, irregular), margin (circumscribed, irregular, spiculated), internal enhancement (homogenous, heterogenous, rim enhancement, dark internal septations) and kinetic curve assessment according to Breast Imaging Reporting and Data System (BI-RADS) criteria of prone MRI [21].

Third-look US using RVS

Third-look US using RVS was performed in the supine and arm-up position [8, 15–17, 22, 23] (Fig. 1a, b). The RVS system consisted of an US scanner, magnetic field generator, magnetic sensor, and workstation with built-in RVS software (FUJIFILM Health care Corporation). The process began with the transfer of breast MRI data, in the Digital Imaging and Communications in Medicine (DICOM) format, to the workstation. Subsequently, the magnetic sensor detected the position and probe motion during the examination by sensing a magnetic field. Next, the 3D position of the probe was transmitted to the workstation, which computed the information regarding the position and displayed the MRI-multi-planar reconstruction image equivalent to the US image on the workstation

monitor. The nipple on the side being examined was used as the reference point for synchronizing the MRI and US images. Correction was made during the examination by checking the location of the lesion compared to the blood vessels, fat, ligaments and mammary glands [9].

RVS-guided biopsy

When MRI-detected lesions were identified with RVS, US-guided biopsy was performed. Core needle biopsy (CNB) was performed with a 16-gauge spring-loaded automatic core needle (Monopty; C.R. Bard, Covington, GA, USA) [20]. If the result of CNB was high-risk atypical ductal hyperplasia, preoperative RVS-guided marking and excisional biopsy were performed; the final histopathological classification was based on this biopsy sample [15]. This examination is contraindicated for patients with pacemakers.

Pathological criteria for invasive ductal carcinoma (IDC) and other special types

IDC subtype was determined according to hormonal receptor (HR) status, Ki-67 status, and HER-2 status [22]. Immunohistochemical staining was performed in the same way even for tissue types other than IDC.

Pathological criteria for ductal carcinoma in situ (DCIS)

DCIS subtype was classified as low-, intermediate-, or high-grade based on the features of the nuclei of the neoplastic cells [24].
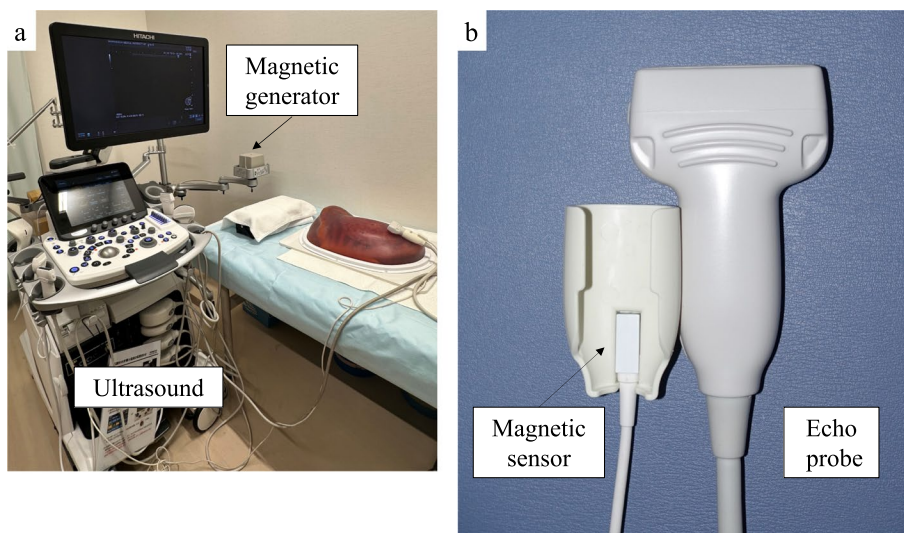
Fig. 1 RVS system equipment in the outpatient clinic (**a**). When performing RVS, the attachment containing the magnetic sensor is fitted into the handle of the probe (**b**). RVS: real-time virtual sonography

Saito *et al. BMC Medical Imaging*   (2024) 24:200

Page 4 of 11

Intramammary distribution of MRI-detected lesions

We divided the distribution of MRI-detected mammary gland lesions located from the skin to the pectoralis major muscle into four regions: adjacent to the superficial mammary fascia (s area), adjacent to the deep mammary fascia (d area), center of the mammary gland (c area), and atrophic mammary gland (a area) (Fig. 2) [16].

Results

This study included 32 women (median age, 57 years; range, 41–73) with 32 lesions (22 mass lesions and 10 focus lesions) detected with MRI but not with second-look conventional B-mode US. Third-look US using RVS was able to detect 27 (84%) of these 32 lesions (19 [86%] of 22 mass lesions and 8 [80%] of 10 focus lesions). The 5 MRI-detected lesions that could not be identified were followed-up annually with third-look US using RVS. No changes were observed in these lesions in one years. Table 1 shows the MRI characteristics of the MRI-detected lesions. Table 2 shows the MRI and US characteristics of the benign and malignant lesions.

The intramammary distribution of benign and malignant lesions is shown in Table 3. Of these, 16 were located around the mammary fascia (9 [33%] in s area and 7 [26%] in d area), 5 (19%) in c area, and 6 (22%) in

a area. Of the 21 lesions not located in a area, where the mammary gland was atrophic and the landmarks were not obvious, 16 (76%) were located around the mammary fascia, i.e., in the marginal part of the mammary gland. Figures 3, 4, 5 and 6 show cases located in each of the four areas.

During this study period, we performed 1426 breast MRI and identified 215 MRI-detected lesions (mass in 119, NME in 76, focus in 18). Regarding MRI-detected mass and focus lesions, we were able to detect 105 lesions by second-look conventional B-mode US and 27 lesions using third-look US using RVS. Second-look conventional B-mode US detected 97 mass lesions and 8 focus lesions. Table 4 shows the distribution of MRI-detected mass and focus lesions. In these MRI-detected mass and focus lesions, 78 (57%) were located around the mammary fascia (42 [31%] were located in s area and 36 [26%] in d area], 46 (34%) in c area and 13 (9%) in a area. In the MRI-detected mass and focus lesions detected by second-look conventional B-mode US, 60 (57%) were located around the mammary fascia (32 [30%] were located in s area and 28 lesions [27%] in d area), 38 lesions (36%) in c area and 7 lesions (7%) in a area. In the MRI-detected mass and focus lesions which couldn't be detected were located in 1 lesion (20%) was
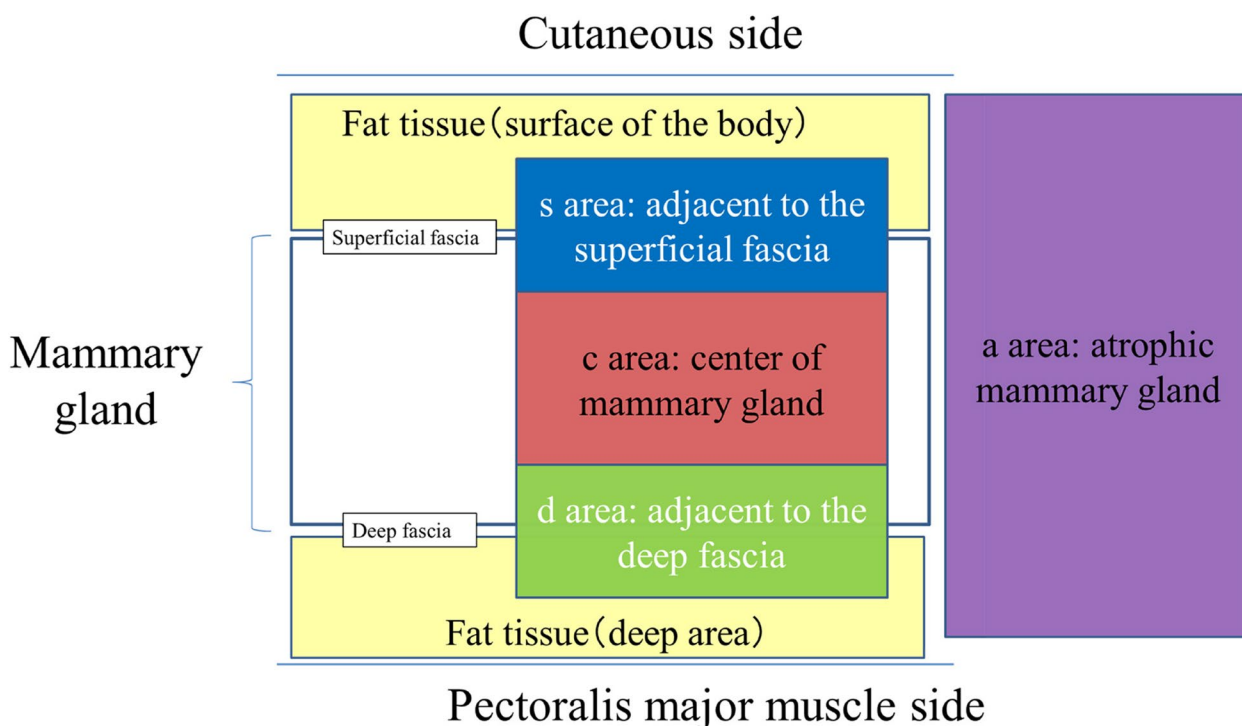
Fig. 2 Intramammary distribution of MRI-detected lesions. We divided the distribution of MRI-detected lesions in the mammary gland as follows: around the superficial mammary fascia (s area), adjacent to the deep mammary fascia (d area), center of mammary gland (c area), and atrophic mammary gland (a area). MRI: magnetic resonance imaging

Saito *et al. BMC Medical Imaging*   (2024) 24:200

Page 5 of 11

Table 1 MRI characteristics of MRI-detected lesions in this study

	RVS correlate (*n* = 27)	No RVS correlate (*n* = 5)
Mean size (mm, range)	6.5 (3.3–17)	6.4 (4.7–7.3)
Lesion type		
Focus	8 (30%)	2 (40%)
Mass	19 (70%)	3 (60%)
Shape		
Oval	14 (52%)	1 (20%)
Round	11 (41%)	4 (80%)
Irregular	2 (7%)	0
Margin		
Circumscribed	25 (93%)	5 (100%)
Irregular	2 (7%)	0
Spiculated	0	0
Internal enhancement		
Homogenous	24 (88%)	5 (100%)
Heterogenous	2 (7%)	0
Rim enhancement	1 (4%)	0
Dark internal septations	0	0
Kinetic curve assesment		
Initial phase		
Slow	0	0
Medium	10 (37%)	0
Fast	15 (55%)	5 (100%)
Unknown	2 (7%)	0
Delayed phase		
Persistent	7 (26%)	2 (40%)
Plateau	12 (44%)	2 (40%)
Washout	6 (22%)	1 (40%)
Unknown	2 (7%)	0

located in s area, 3 lesions (60%) in c area and 1 lesion (20%) in d area.

We were able to perform RVS-guided biopsy of all 27 lesions detected by third-look US using RVS. CNB and excisional biopsy were performed, respectively, in 17 (63%) and 10 (37%) of the 27 lesions overall. This corresponded to 13 (68%) and 6 (32%) of the 19 mass lesions and 4 (50%) and 4 (50%) of the 8 focus lesions, respectively. Of the 27 lesions, 8 (30%) were malignant, which consisted of 5 of 19 (26%) mass lesions and 3 of 8 (38%) focus lesions.

The histopathological results of the malignant lesions were IDC (luminal A) in three lesions (all focus lesions), IDC (luminal B) in one mass lesion, and DCIS (low-grade) in four (all mass lesions). The histopathological results of benign lesions were mastopathy in 3, intraductal papilloma in 2, atypical ductal hyperplasia in 1, atypical lobular hyperplasia and hemangioma in 1, and other in 12. Malignant lesions were located in all areas:

around the mammary fascia in 63% (s area in 3 [38%] lesions, d area in 2 [25%] lesions), c area in 1 (13%) lesion, and a area in 2 (25%) lesions.

Discussion

In this study, 27 (84%) of 32 MRI-detected mass and focus lesions were able to be detected by third-look US using RVS. Of these 27 lesions, 16 were around the mammary fascia (9 [33%] in s area and 7 [26%] in d area), 5 (19%) were in c area, and 6 (22%) were in a area. Malignant lesions were present in all areas. During this study period, 132 MRI-detected mass and focus lesions were identified. In these MRI-detected lesions, 78 (57%) were located around the mammary fascia (42 [31%] were located in s area and 36 [26%] in d area), 46 (34%) in c area and 13 (9%) in a area. In these MRI-detected lesions detected by second-look conventional B-mode US, 60 (57%) were located around the mammary fascia (32 [30%] were located in s area and 28 lesions [27%] in d area), 38 lesions (36%) in c area and 7 lesions (7%) in a area. We consider that adequate attention should be paid to the whole mammary gland when we perform third-look US using MRI/US fusion technique.

While second-look US is inexpensive, radiation-free, and useful for identifying breast lesions detected with MRI, several studies found wide variation in the general detection rate for second-look US, ranging from 59% to 86.8% [7–11]. Other authors have noted that findings on second-look US were subtle, necessitating careful scanning techniques for successful MRI/US correlation [9, 25]. Ultrasound scanning of the breast was performed with special attention to the area of the detected enhancing lesion using MR images as a guide [25]. Furthermore, there is no direct evidence that lesions detected on MRI can be detected and biopsied accurately [8] whereas no special US operator skill or experience is needed to perform RVS. In terms of objectivity and reproducibility, third-look US with MRI/US fusion techniques is considered superior to second-look conventional B-mode US [7, 8, 15–17, 20, 22, 23, 26–30].

Differences in posture between examinations in supine versus prone position cause lesion displacement. Aribal et al. reported that an abbreviated supine sequence following a standard prone dynamic contrast-enhanced diagnostic MRI with one administration of contrast was useful for identifying lesion locations [31]. Breast size and lesion displacement relative to the distance from the sternum or nipple were not correlated [31]. Carbonaro et al. [19] reported that prone MRI resulted in lesion displacement of 30–60 mm in three orthogonal directions relative to supine MRI. Considering that the mean position error for RVS is approximately 12 mm, morphological findings can be directly compared between US and supine MRI

Saito *et al. BMC Medical Imaging*   (2024) 24:200

Page 6 of 11

Table 2 MRI and US characteristics of benign lesions and malignant lesions in this study

	Total (= 27)	Benign (n = 19)	Malignant (n = 8)
Mean size (mm, range)	6.5 (3.3–17)	6.2 (3.8–10)	7.3 (3.3–17)
Lesion type			
Focus	8	5 (26%)	3 (38%)
Mass	19	14 (74%)	5 (63%)
Shape			
Oval	14	10 (53%)	4 (50%)
Round	11	8 (42%)	3 (38%)
Irregular	2	1(5%)	1 (13%)
Margin			
Circumscribed	25	18 (95%)	7 (88%)
Irregular	2	1 (5%)	1 (13%)
Spiculated		0	0
Internal enhancement			
Homogenous	24	17 (89%)	7 (88%)
Heterogenous	2	2 (11%)	0
Rim enhancement	1	0	1 (13%)
Dark internal septations		0	0
Kinetic curve assesment			
Initial phase			
Slow	0	0	0
Medium	10	7 (37%)	3 (38%)
Fast	15	10 (53%)	5 (63%)
Unknown	2	2 (11%)	0
Delayed phase			
Persistent	7	6 (32%)	1 (13%)
Plateau	12	7 (37%)	5 (63%)
Washout	6	4 (21%)	2 (25%)
Unknown	2	2 (11%)	0
Shape (sonography)			
Oval	14	11 (58%)	3 (38%)
Round	9	7 (37%)	2 (25%)
Irregular	4	1 (5%)	3 (38%)
Orientation (sonography)			
Parallel	23	18 (95%)	5 (63%)
Non-parallel	4	1 (5%)	3 (38%)
Margin (sonography)			
Circumscribed	23	18 (95%)	5 (63%)
Non-circumscribed	4	1 (5%)	3 (38%)
Lesion Boundary (sonography)			
Abrupt interphase	27	19 (100%)	8 (100%)
Echogenic halo	5	0	5 (63%)
Echo pattern (sonography)			
Hypoechoic	19	14 (74%)	5 (63%)
Isoechoic	8	5 (26%)	3 (38%)
Intramammary distribution			
Around mammary fasia (s and d areas)	16	11 (58%)	5 (63%)
Center of mammary gland (c area)	5	4 (21%)	1 (13%)
Atrophic mammary gland (a area)	6	4 (21%)	2 (25%)

**Table 3** Intramammary distribution of benign and malignant lesions

	Benign lesions (*n* = 19)	Malignant lesions (*n* = 8)
Intramammary distribution		
s area	6 (32%)	3 (38%)
c area	4 (21%)	1 (13%)
d area	5 (26%)	2 (25%)
a area	4 (21%)	2 (25%)

[17]. Moreover, RVS provides accurate information about position even in the absence of landmarks identified with US and MRI. Recent studies have demonstrated the utility of second-look US using RVS that synchronizes supine MRI and US images with respect to the nipple on the side being examined [9, 32]. In addition to the nipple, spatial location of tumor and blood vessels, Cooper's ligament, adipose tissue, and glandular tissue have been reported to be usable as landmark [9]. Also, because the mammary glands are fatty and easily deformed, manipulation of the ultrasound probe and respiratory movement cause misalignment between the ultrasound image and the MRI-multi-planar reconstruction image. Therefore, the technique to minimize misalignment is to scan the probe gently so as not to compress the breast [17]. We believe these landmarks and techniques enable us to perform biopsies of MRI-detected lesions more accurately.

In this study, the RVS-guided biopsy detection rate for malignant lesions was 30%. According to the BI-RADS classification system [21], the rate with MRI-guided biopsy is 20–50%. Thus, RVS-guided biopsy can be a promising substitute for MRI-guided breast biopsy, but further study is needed.

MRI-guided biopsy is challenging because of various technical issues [33, 34]. First, it is expensive and time-consuming, for patients and radiologists alike. Second, it requires specialized equipment [35]. In contrast, special equipment is not needed for RVS-guided biopsy [9]. Furthermore, the average turnaround time for RVS-guided biopsy is 25 min, which is shorter than the turnaround time for MRI-guided biopsy because the supine breast MRI protocol used in RVS can be shortened [9]. The average time of MRI-guided biopsy was reported about 1 h [36, 37]. The increased use of RVS relative to MRI might be beneficial in terms of time and availability. RVS can also help determine whether an MRI-guided biopsy is absolutely necessary. Performing
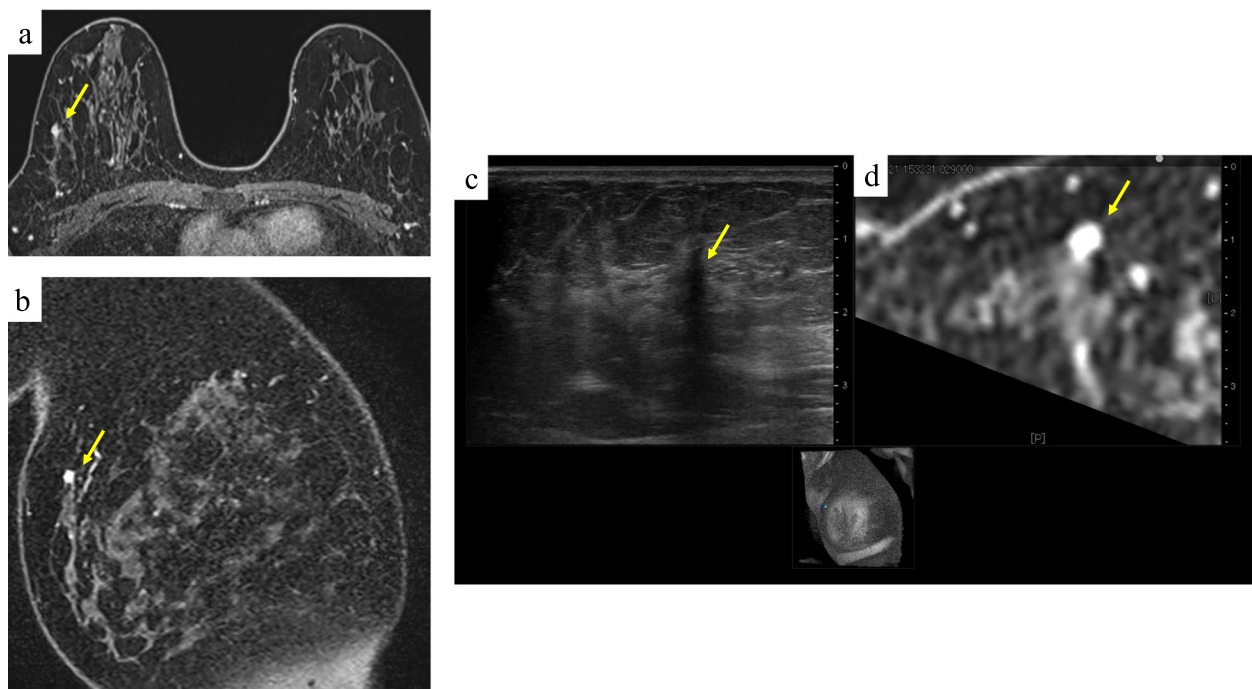
Fig. 3 MRI-detected lesion located in s area. We showed the lesion by an arrow. The patient was a premenopausal woman. Preoperative breast MRI showed a focus lesion with a diameter of 4.0 mm (**a**). After supine MRI (**b**), we performed third-look US using RVS. The image b shows a supine MRI MIP image. RVS displayed early-phase MRI–MPR (**d**), which corresponded to the US image (**c**). We were able to detect the lesion with RVS and perform excisional biopsy. The diagnosis was IDC and the subtype was luminal A. MIP: maximum intensity projection, MPR: multiplanar reconstruction; IDC: invasive ductal carcinoma
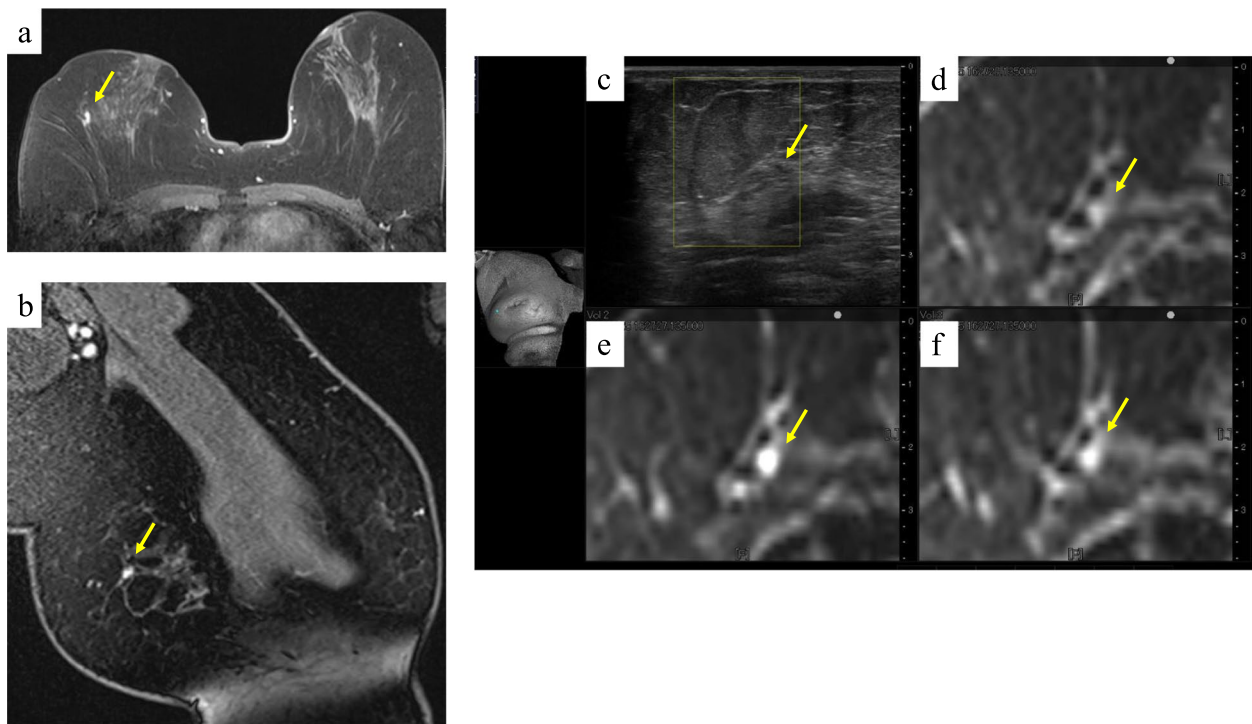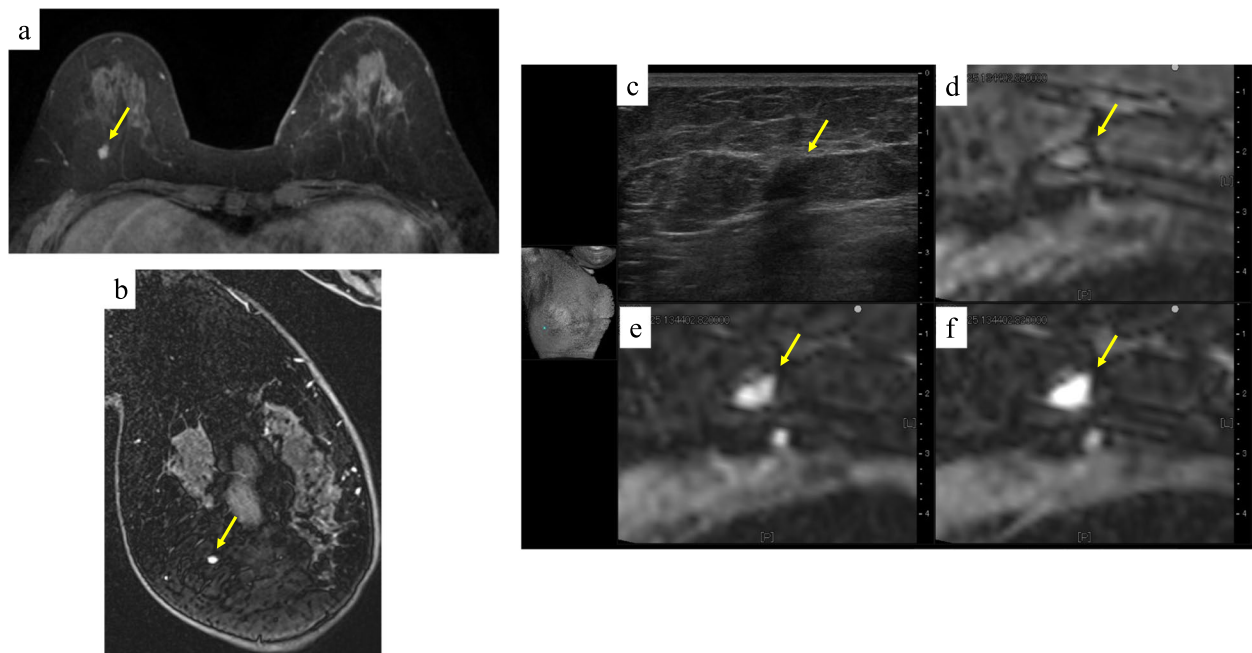
Fig. 4 MRI-detected lesion located in c area. We showed the lesion by an arrow. The patient was a premenopausal woman. Preoperative breast MRI showed a mass lesion with a diameter of 9.4 mm (**a**). After supine MRI (**b**), we performed third-look US using RVS. The image b shows a supine MRI MIP image. RVS displayed the US image (**c**) and which was corresponded to pre-contrast-phase (**d**), early-phase (**e**), and late-phase MRI–MPR (**f**). We were able to detect the lesion with RVS and perform excisional biopsy. The diagnosis was low-grade DCIS. DCIS: ductal carcinoma in situ
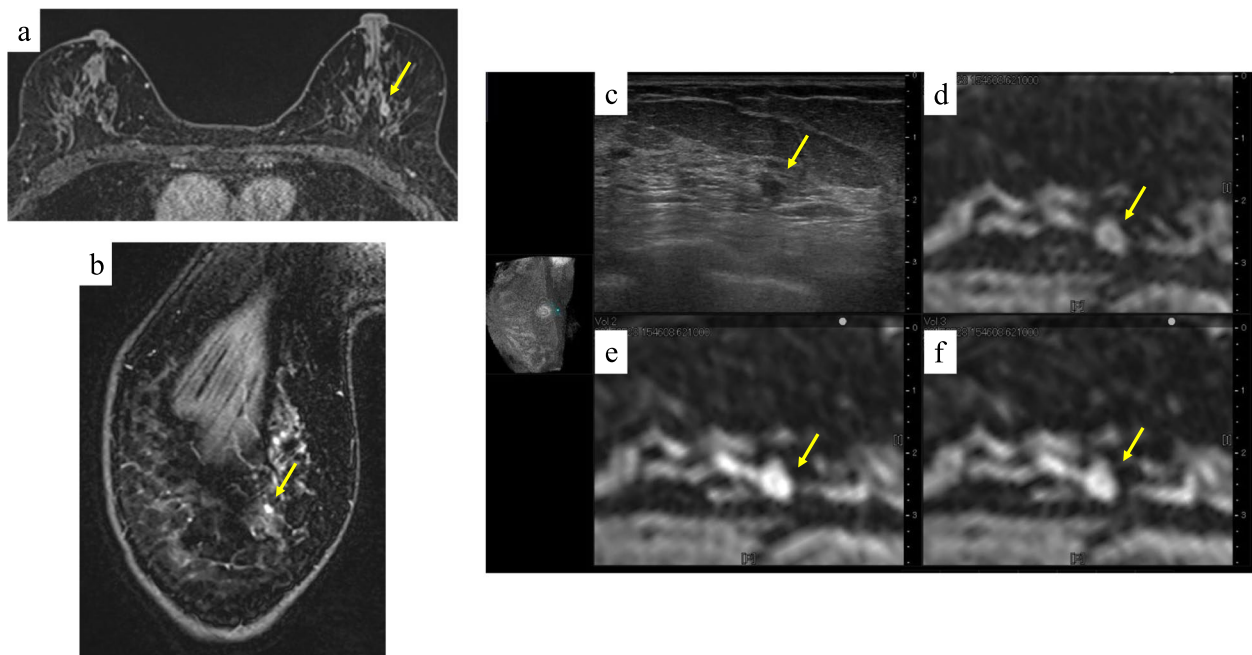
Fig. 5 MRI-detected lesion located in d area. We showed the lesion by an arrow. The patient was a postmenopausal woman. Preoperative breast MRI showed a mass lesion with a diameter of 5.8 mm (**a**). After supine MRI (**b**), we performed third-look US using RVS. The image b shows a supine MRI MIP image. RVS displayed the US image (**c**) and which was corresponded to pre-contrast-phase (**d**), early-phase (**e**), and late-phase MRI–MPR (**f**). We were able to detect this lesion with RVS and perform CNB. The diagnosis was low-grade DCIS. CNB: core needle biopsy

Saito *et al. BMC Medical Imaging* (2024) 24:200

Page 9 of 11

Fig. 6 MRI-detected lesion located in a area. We showed the lesion by an arrow. The patient was a premenopausal woman. Preoperative breast MRI showed a mass lesion with a diameter of 5.8 mm (**a**). After supine MRI (**b**), we performed third-look US using RVS. The image b shows a supine MRI MIP image. RVS displayed the US image (**c**) and which was corresponded to pre-contrast-phase (**d**), early-phase (**e**), and late-phase MRI–MPR (**f**). We were able to detect this lesion with RVS and performed CNB. The lesion was benign

Table 4 Intramammary distribution of MRI-detected mass and focus lesions during this study period

	All lesions	Second-look conventional B-mode US correlate	Third-look US using RVS correlate	No second-look conventional B-mode US and third-look US using RVS correlate
s area	42 (31%)	32 (30%)	9 (33%)	1 (20%)
c area	46 (34%)	38 (36%)	5 (19%)	3 (60%)
d area	36 (26%)	28 (27%)	7 (26%)	1 (20%)
a area	13 (9%)	7 (7%)	6 (22%)	0
total	137	105	27	5

third-look US using RVS needs supine MRI. Performing additional supine MRI costs the patient but this study didn't compare the costs of MRI-guided biopsy with those of RVS-guided biopsy.

This study had several limitations. First, it was a retrospective investigation with a relatively small number of patients. Additional prospective studies with more patients are needed. Second, supine breast MRI using a body surface coil is affected by artifacts related to movements during breathing as well as heartbeats. Low coil filling factor leads to poor image quality. Therefore, it is not a firmly established method to diagnose breast cancer. Additional research should be performed to evaluate the accuracy of the method.

Conclusions

Third-look US using RVS was able to detect 84% of MRI-detected mass and focus lesions that could not be identified with second-look conventional B-mode US. It was used to evaluate the intramammary distribution of these lesions. 59% of MRI-detected mass or focus lesions detected by third-look US using RVS and 57% of MRI-detected lesions detected by second-look conventional-B mode US were located around the mammary fascia, where the contrast with the surrounding tissue was small. Malignant lesions were present in all areas. MRI-detected lesions were distributed in all areas in the mammary gland. We consider that adequate attention should be paid to the whole mammary gland when we perform

Saito *et al. BMC Medical Imaging*   (2024) 24:200

Page 10 of 11

third-look US using RVS for mass and focus lesions detected by MRI.

Abbreviations

MRI	Magnetic resonance imaging
US	Ultrasound
RVS	Real-time virtual sonography
NME	Non-mass enhancement
BI-RADS	Breast imaging reporting and data system
DICOM	Digital imaging and communications in medicine
CNB	Core needle biopsy
IDC	Invasive ductal carcinoma
ILC	Invasive lobular carcinoma
HR	Hormonal receptor
DCIS	Ductal carcinoma in situ

Declarations

Ethics approval and consent to participate
This preliminary retrospective study was approved by the institutional review board of Aichi Medical University Hospital (approval number, 2022–125). Standard written informed consent was obtained at the time of the procedure. The need for informed consent was waived for this retrospective study. All procedures were performed in accordance with the ethical standards of the responsible committee on human experimentation (institutional and national) and with the Helsinki Declaration of 1964 and later versions.

Consent for publication
Not applicable.

Competing interests
The authors declare no competing interests.

Author details
[1]Division of Breast and Endocrine Surgery, Department of Surgery, Aichi Medical University, 1-1 Yazakokarimata, Nagakute-City, Aichi 480-1195, Japan. [2]Department of Radiology, Aichi Medical University, 1-1 Yazakokarimata, Nagakute-City, Aichi 480-1195, Japan.

References
1. Kuhl CK. Current status of breast MR imaging. Part 2. Clinical applications. Radiology. 2007;244(3):672–91.
2. Morris EA. Diagnostic breast MR imaging: current status and future directions. Radiol Clin North Am. 2007;45(5):863–80 vii.
3. Burki TK. Preoperative MRI in breast cancer. Lancet Oncol. 2015;16(15):e530.
4. Parsyan A, Moldoveanu D, Balram B, Wong S, Zhang DD, Svadzian A, et al. Influence of preoperative magnetic resonance imaging on the surgical management of breast cancer patients. Am J Surg. 2016;211(6):1089–94.
5. Debald M, Abramian A, Nemes L, Dobler M, Kaiser C, Keyver-Paik MD, et al. Who may benefit from preoperative breast MRI? A single-center analysis of 1102 consecutive patients with primary breast cancer. Breast Cancer Res Treat. 2015;153(3):531–7.
6. Houssami N, Ciatto S, Macaskill P, Lord SJ, Warren RM, Dixon JM, et al. Accuracy and surgical impact of magnetic resonance imaging in breast cancer staging: systematic review and meta-analysis in detection of multifocal and multicentric cancer. J Clin Oncol. 2008;26(19):3248–58.
7. Fausto A, Bernini M, La Forgia D, Fanizzi A, Marcasciano M, Volterrani L, et al. Six-year prospective evaluation of second-look US with volume navigation for MRI-detected additional breast lesions. Eur Radiol. 2019;29(4):1799–808.
8. Watanabe R, Ando T, Osawa M, Ido M, Kousaka J, Mouri Y, et al. Second-look US using real-time virtual sonography, a coordinated breast US and MRI system with electromagnetic tracking technology: A pilot study. Ultrasound Med Biol. 2017;43(10):2362–71.
9. Uematsu T, Takahashi K, Nishimura S, Watanabe J, Yamasaki S, Sugino T, et al. Real-time virtual sonography examination and biopsy for suspicious breast lesions identified on MRI alone. Eur Radiol. 2016;26(4):1064–72.
10. Hong MJ, Cha JH, Kim HH, Shin HJ, Chae EY, Shin JE, et al. Second-look ultrasonography for MRI-detected suspicious breast lesions in patients with breast cancer. Ultrasonography. 2015;34(2):125–32.
11. Cheung JY, Moon JH. Follow-up design of unexpected enhancing lesions on preoperative MRI of breast cancer patients. Diagn Interv Radiol. 2015;21(1):16–21.
12. Dratwa C, Jalaguier-Coudray A, Thomassin-Piana J, Gonin J, Chopier J, Antoine M, et al. Breast MR biopsy: Pathological and radiological correlation. Eur Radiol. 2016;26(8):2510–9.
13. Park HL, Hong J. Vacuum-assisted breast biopsy for breast cancer. Gland Surg. 2014;3(2):120–7.
14. Spick C, Schernthaner M, Pinker K, Kapetas P, Bernathova M, Polanec SH, et al. MR-guided vacuum-assisted breast biopsy of MRI-only lesions: a single center experience. Eur Radiol. 2016;26(11):3908–16.
15. Nakano S, Yoshida M, Fujii K, Yorozuya K, Mouri Y, Kousaka J, et al. Fusion of MRI and sonography image for breast cancer evaluation using real-time virtual sonography with magnetic navigation: first experience. Jpn J Clin Oncol. 2009;39(9):552–9.
16. Nakano S, Kousaka J, Fujii K, Yorozuya K, Yoshida M, Mouri Y, et al. Impact of real-time virtual sonography, a coordinated sonography and MRI system that uses an image fusion technique, on the sonographic evaluation of MRI-detected lesions of the breast in second-look sonography. Breast Cancer Res Treat. 2012;134(3):1179–88.
17. Nakano S, Yoshida M, Fujii K, Yorozuya K, Kousaka J, Mouri Y, et al. Real-time virtual sonography, a coordinated sonography and MRI system that uses magnetic navigation, improves the sonographic identification of enhancing lesions on breast MRI. Ultrasound Med Biol. 2012;38(1):42–9.
18. Satake H, Ishigaki S, Kitano M, Naganawa S. Prediction of prone-to-supine tumor displacement in the breast using patient position change: investigation with prone MRI and supine CT. Breast Cancer. 2016;23(1):149–58.
19. Carbonaro LA, Tannaphai P, Trimboli RM, Verardi N, Fedeli MP, Sardanelli F. Contrast enhanced breast MRI: spatial displacement from prone to supine patient's position. Preliminary Results Eur J Radiol. 2012;81(6):e771–4.
20. Goto M, Nakano S, Saito M, Banno H, Ito Y, Ido M, et al. Evaluation of an MRI/US fusion technique for the detection of non-mass enhancement of breast lesions detected by MRI yet occult on conventional B-mode second-look US. J Med Ultrason (2001). 2022;49(2):269–78.
21. Morris EA, Comstock CE, Lee CH, et al. ACR BI-RADS® Magnetic Resonance Imaging. In: ACR BI-RADS® Atlas, Breast Imaging Reporting and Data System. Reston: American College of Radiology; 2013.
22. Ando T, Ito Y, Ido M, Osawa M, Kousaka J, Mouri Y, et al. Pre-operative planning using real-time virtual sonography, an MRI/Ultrasound image fusion technique, for breast-conserving surgery in patients with non-mass enhancement on breast MRI: A preliminary study. Ultrasound Med Biol. 2018;44(7):1364–70.
23. Nakano S, Ando T, Tetsuka R, Fujii K, Yoshida M, Kousaka J, et al. Reproducible surveillance breast ultrasound using an image fusion technique in

Saito *et al. BMC Medical Imaging*   (2024) 24:200

Page 11 of 11

a short-interval follow-up for BI-RADS 3 lesions: a pilot study. Ultrasound Med Biol. 2014;40(6):1049–57.

24. Komforti MK, Harmon BE. Educational Case: Ductal Carcinoma In Situ (DCIS). Acad Pathol. 2019;6:2374289519888727.

25. Abe H, Schmidt RA, Shah RN, Shimauchi A, Kulkarni K, Sennett CA, et al. MR-directed ("Second-Look") ultrasound examination for breast lesions detected initially on MRI: MR and sonographic findings. AJR Am J Roentgenol. 2010;194(2):370–7.

26. Aribal E, Tureli D, Kucukkaya F, Kaya H. Volume navigation technique for ultrasound-guided biopsy of breast lesions detected only at MRI. AJR Am J Roentgenol. 2017;208(6):1400–9.

27. Fausto A, Fanizzi A, Volterrani L, Mazzei FG, Calabrese C, Casella D, et al. Feasibility, Image Quality and Clinical Evaluation of Contrast-Enhanced Breast MRI Performed in a Supine Position Compared to the Standard Prone Position. Cancers (Basel). 2020;12(9). https://doi.org/10.3390/cancers12092364.

28. Uematsu T. Real-time virtual sonography (RVS)-guided vacuum-assisted breast biopsy for lesions initially detected with breast MRI. Jpn J Radiol. 2013;31(12):826–31.

29. Fausto A, Rizzatto G, Preziosa A, Gaburro L, Washburn MJ, Rubello D, et al. A new method to combine contrast-enhanced magnetic resonance imaging during live ultrasound of the breast using volume navigation technique: a study for evaluating feasibility, accuracy and reproducibility in healthy volunteers. Eur J Radiol. 2012;81(3):e332–7.

30. Kucukkaya F, Aribal E, Tureli D, Altas H, Kaya H. Use of a volume navigation technique for combining real-time ultrasound and contrast-enhanced MRI: Accuracy and feasibility of a novel technique for locating breast lesions. AJR Am J Roentgenol. 2016;206(1):217–25.

31. Aribal E, Bugdayci O. Supplementary abbreviated supine breast MRI following a standard prone breast MRI with single contrast administration: is it effective in detecting the initial contrast-enhancing lesions? Diagn Interv Radiol. 2019;25(4):265–9.

32. Kang DK, Jung Y, Han S, Kim JY, Kim TH. Clinical Utility of Real-Time MR-navigated ultrasound with supine breast MRI for suspicious enhancing lesions not identified on second-look ultrasound. Ultrasound Med Biol. 2017;43(2):412–20.

33. Brennan SB. Breast magnetic resonance imaging for the interventionalist: magnetic resonance imaging-guided vacuum-assisted breast biopsy. Tech Vasc Interv Radiol. 2014;17(1):40–8.

34. Price ER. Magnetic resonance imaging-guided biopsy of the breast: fundamentals and finer points. Magn Reson Imaging Clin N Am. 2013;21(3):571–81.

35. Nakashima K, Uematsu T, Harada TL, Takahashi K, Nishimura S, Tadokoro Y, et al. MRI-detected breast lesions: clinical implications and evaluation based on MRI/ultrasonography fusion technology. Jpn J Radiol. 2019;37(10):685–93.

36. Noroozian M, Gombos EC, Chikarmane S, Georgian-Smith D, Raza S, Denison CM, et al. Factors that impact the duration of MRI-guided core needle biopsy. AJR Am J Roentgenol. 2010;194(2):W150–7.

37. Shimoda M, Kim SJ, Tokuda Y, Sota Y, Miyake T, Tanei T, et al. Effect of Computer-aided Detection System Use on the Duration of MRI-guided Biopsy of the Breast. Anticancer Res. 2020;40(11):6437–41.

Publisher's Note